SAND94-0175C
CONF-940553--10

A COMPARISON OF SPENT FUEL SHIPPING CASK RESPONSE TO 10 CFR 71 NORMAL CONDITIONS AND REALISTIC HOT DAY EXTREMES

Steven James Manson
The University of Texas at Austin
College of Engineering
Austin, TX 78712
(512) 471-3119

Steven Eric Gianoulakis
Sandia National Laboratories
Mail Stop 0835
Albuquerque, NM 87185
(505) 844-0450

ABSTRACT

The structural properties of spent nuclear fuel shipping containers vary as a function of the cask wall temperature. An analysis is performed to determine the effect of a realistic, though bounding, hot day environment on the thermal behavior of spent fuel shipping casks. These results are compared to those which develop under a steady-state application of the prescribed normal thermal conditions of 10CFR71. The completed analysis revealed that the majority of wall temperatures, for a wide variety of spent fuel shipping cask configurations, fall well below those predicted by using the steady-state application of the regulatory boundary conditions. It was found that maximum temperatures at the cask surface occasionally lie above temperatures predicted under the regulatory condition. This is due to the conservative assumptions present in the ambient conditions used. The analysis demonstrates that diurnal temperature variations which penetrate the cask wall have maxima substantially less than the corresponding temperatures obtained when applying the steady-state regulatory boundary conditions. Therefore, it is certain that vital cask components and the spent fuel itself will not exceed the temperatures calculated by use of the steady-state interpretation of the 10CFR71 normal conditions.

I. INTRODUCTION

The U. S. Nuclear Regulatory Commission (NRC) has specified the normal thermal conditions under which spent fuel shipping containers are to be evaluated in Title 10 of the Code of Federal Regulations, Section 71 (10CFR71). The regulation specifies an ambient temperature of 38 °C (100 °F), and a daily total insolation of 800 cal/cm^2, which is to be deposited over a twelve hour period. One frequently used interpretation of the insolation regulation assumes that the solar flux is steady, at a rate of 67 cal/cm^2/hr. As the specified ambient temperature and steady-state solar flux are somewhat lower than peaks often reached in some regions of the country, it has been deemed valuable to compare the effects of an hourly varying *realistic*, though bounding (see Section II), ambient cycle to those of the regulation as implemented. This study will undertake a comparison of cask response to two sets of ambient conditions, and examine two different realistic cask designs in order to draw conclusions about the general differences between the regulatory and realistic conditions.

Previous studies by Lake have shown that the NRC's hot day thermal condition is adequate for predicting the thermal response of the interior regions of large *water-cooled* shipping casks.[1] It has also been shown by Brown that the thermal response of the surface regions of casks characterized as simple steel plates are reasonably well represented by utilization of the normal condition of 10CFR71.[2] Actual cask designs, however, are laminations of several concentric shells with widely varying thermal properties, and hence much more complicated than the steel plates studied by Brown. Furthermore, the studies by Lake and Brown use only simple mathematical functions to represent postulated environmental data. It is thought that by utilizing *actual* hot day data, a more realistic analysis may be performed. Lastly, Brown's analysis used a lumped-parameter model. It is felt that more exact conclusions may be drawn by modeling the spatial propagation of thermal effects through the cask wall, especially in situations involving multiple layers of cask material.

The important difference between the regulations as cited, and the actual typical meteorological conditions, is two-fold. First, there is the matter of the peak values of temperature and insolation, which both may be potentially larger than the stated regulatory condition. Second, the nature of the diurnal variation of both the temperature and

This work was supported by the United States Department of Energy under Contract DE-AC04-94AL85000.

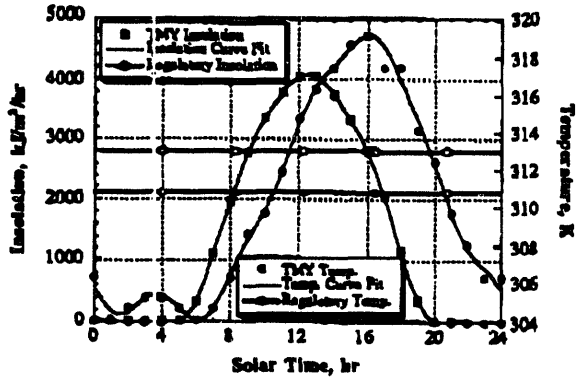

Figure 1: TMY Hot Day Data

insolation rate suggests that transient thermal behavior not predicted by the steady-state interpretation of the regulatory model may occur. These effects compete to a certain extent, and detailed analysis can quantify the overall thermal behavior of transport casks subjected to diurnal variations in ambient conditions.

It is crucial to point out that the analyses described herein have been carried out with very realistic ambient conditions and cask designs. The heat load emanating from the spent fuel will not change the relative profiles of the realistic and regulatory cases even if the heat load is varied drastically. However, variation of the heat source will change the magnitudes of the temperatures within the cask walls quite significantly. Thus, it must be noted that the temperature profiles calculated for discussion in this section are to be viewed only with regard to comparisons of the relative effects of the realistic and regulatory conditions, and should not in any way be construed as predictions of actual *temperatures* in transport situations. Therefore, if any specific temperature within any cask wall is shown as exceeding the specific regulatory guidelines for the temperatures of corresponding cask components, this must not be taken as a weakness of the cask design, the computational algorithm, or of this analysis. The calculations which demonstrate compliance with specific temperature regulations are the domain of cask manufacturers and are outside the scope of this report.

II. DESCRIPTION OF THE WORK

The meteorological data which was used in this study has been compiled by the National Climatic Data Center (NCDC). The NCDC has gathered weather data from all over the U.S. over a period of 27 years and combined it in a series of records cumulatively referred to as the Typical Meteorological Year (TMY)[3]. The data of specific concern for this study are the solar radiation measurements and the temperature. The characterization of insolation and temperature together will allow the adequate formulation of a thermal boundary condition for the surface of a cask.

All available TMY data were searched in order to locate each day in which the integrated radiation flux (total fluence) was a maximum. A similar search was conducted to find the maximum temperature in the U. S. TMY. The worst case day for insolation in the TMY data was found to be for Dodge City, Kansas, on May 29 (834.4 cal/cm^2). The hottest day in the TMY was recorded for Yuma, Arizona, on July 10 (t_{max} = 46 °C). The TMY data for these days are shown in Figure 1.

The measurements provided in the TMY data sets are recorded in hourly increments, however, a *realistic* thermal simulation which utilizes this data will have a time step smaller than one hour. It becomes necessary to interpolate the data in some manner, in order to provide insolation or temperature boundary conditions at any instant over the course of a day. There is an abundance of interpolation routines which may prove useful for the present application. However, due to the general shape of the data, the Cosine Fourier Transformation (CFT) was chosen for use in evaluating the data. The CFT is particularly suitable due to its inherent ability to evaluate the derivative of a function once CFT of the function is known.[4] This ability is helpful when evaluating the insolation data, since the TMY data provides measurements of the insolation fluence during each hour previous to the recording of the measurement, which is effectively the integral of the radiation flux. Thus, the insolation rate may be recovered from the data by taking the derivative of the fluence value. The CFT curve fits of the TMY data are also shown in Figure 1.

The CFT function of temperature has been smoothed in order to eliminate the small order oscillations present in the data. The peak temperature has been preserved, as well as the general form of the diurnal variation, however, smaller oscillations which do not contribute to the general, overall diurnal behavior are eliminated. Had the small oscillations been retained, physically unrealistic "wiggles" in the CFT interpolation would have resulted. The smoothing was performed by canceling 20 (out of 48) of the higher order terms of the CFT by setting their coefficients equal to zero. These coefficients correspond to cosine waves with the smallest periods, and hence are most responsible for the extremely localized "wiggling."

A. Heat Conduction Model

In order to determine the penetrative effects of the diurnal variation of temperature and insolation, and thereby the maximum temperature profile through the cask wall, it was necessary to formulate an appropriate transient heat conduction model. The model accurately represents the geometry of interest, is one-dimensional and time accurate. A complete description of the

numerical model may be found in the report which was the foundation of this paper.[5]

The general one-dimensional transient heat conduction equation in cylindrical coordinates is given as[6]:

$$\frac{1}{r}\frac{\partial}{\partial r}\left(r k_r \frac{\partial t}{\partial r}\right) + q''' = \rho c_p \frac{\partial t}{\partial \tau} \qquad 1$$

In this notation, t is temperature, τ is time, r is the spatial coordinate, k_r is the thermal conductivity as a function of r, q''' is the generation term, ρ is the material density, and c_p is the material specific heat.

For regions away from material interfaces, where k_r, ρ and c_p can be treated as constants and with no generation term, the expression may be simplified using the thermal diffusivity, $\alpha = k/(\rho c_p)$, and the definition of the LaPlacian, in the radial coordinate. Equation 1 becomes:

$$\frac{\partial^2 t}{\partial r^2} + \frac{1}{r}\frac{\partial t}{\partial r} = \frac{1}{\alpha}\frac{\partial t}{\partial \tau} \qquad 2$$

Discretization of this equation yields:

$$\frac{t_{i+1} - 2t_i + t_{i-1}}{\Delta r_i^2} + \frac{1}{r_i}\frac{t_{i-1} - t_{i+1}}{2\Delta r_i} = \frac{1}{\alpha}\frac{t_i - t_i^{old}}{\Delta \tau} \qquad 3$$

This expression can be solved by a tridiagonal matrix algorithm. The tridiagonal matrix solution algorithm is well documented,[4] and can be implemented successively for transient solutions of Equation 3 on the interior domain of any layer.

As the computational model is transient and one-dimensional, it is necessary to define two boundary conditions in addition to an initial condition. The initial condition is arbitrary because the solution is periodic, thus the simulation continues until all residual effects of the initial condition have died away. The interior boundary condition is a known constant heat flux, q_g'', which appears due to the spent nuclear fuel inside the cask. The external boundary condition is formulated from the realistic bounding environmental data. The outer surface of the spent fuel shipping cask is exposed to a diurnally varying ambient temperature, t_∞, which causes convective heat transfer as well as thermal radiation. Furthermore, the surface absorbs incident solar radiation which along with t_∞ is directly available from the TMY data.

Together the equations for the interior nodes and boundary nodes constitute a complete set of governing equations. When these equations are solved simultaneously over time, they yield the transient temperature distribution throughout the cask wall. Once the governing equations have been solved for a twenty-four hour transient, the entire temperature profile in the wall at midnight is compared to that profile which occurred twenty-four hours earlier. This allows the determination of whether the transient solution has become truly periodic. Periodicity will always develop due to the twenty-four hour periodic cycle imposed by the boundary conditions. When the maximum variation in temperature, from midnight to midnight, at every node is less than a specified convergence criterion, a steady periodic solution is said to have been reached. When this occurs, the code post processes the solution data. If steady periodicity has not yet been achieved, the code returns to increment the time step again and calculate the variation for the next whole day.

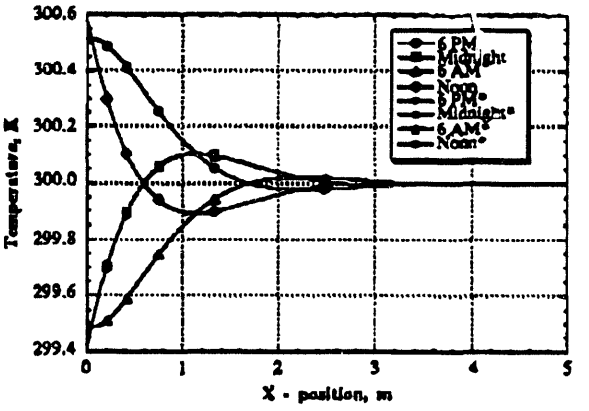

Figure 2: Plot of Numerical and Analytical(*) Solutions of the Benchmark Problem

B. Validation and Benchmarking

The computational procedure was verified to ensure the correctness of its derivation, as well as its implementation. The benchmark problem concerns a semi-infinite slab exposed to convection heat transfer, the ambient temperature, t_∞, varying sinusoidally with a given period, ω. An analytical expression for the temperature variation within the slab exists as a function of time and distance into the slab. Given the ambient temperature, t_∞, and the convection coefficient, h, as well as the material properties of the slab, k and α, the temperature response in the slab after some finite time, $\Delta\tau$, may be calculated from an analytically derived formula at any time in the periodic transient. This benchmark problem was chosen because it is similar to the complex spent fuel container analysis and yet it has a known exact analytical solution.

In this simulation, the semi-infinite slab (a cylinder with an infinite radius) is exposed for a long period of time to a fluid whose temperature, t_∞ is sinusoidally varying with time. The equation representing this temperature oscillation is defined as:

$$t_\infty(\tau) = \bar{t} + t_a \cos(\omega\tau) \qquad 4$$

The amplitude of the variation is given as t_a, and its frequency is ω. The slab is initially at the mean temperature of the fluid, $\bar{t}$ throughout, so that the transient temperature approaches a constant value of $\bar{t}$ as x approaches infinity, irrespective of time. The expected solution is a sinusoidally varying temperature, whose

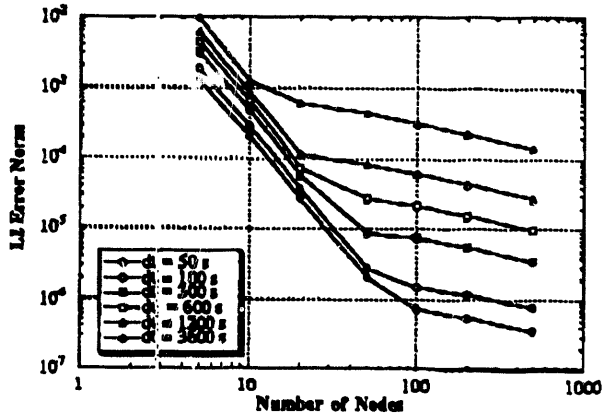

Figure 3: L_1 Error Norm as a Function of Spatial Discretization for Various Time Steps

amplitude decays with position in the slab. Furthermore, the sinusoidal behavior at the surface of the slab should exhibit a phase lag behind the ambient temperature.

Gebhart presents the analytical solution to the problem,[6] one representation of which is presented in Figure 2. The temperature solution as a function of time, τ, x position, and the frequency of the oscillation, ω, is:

$$t(x,\tau) = \bar{t} + \frac{a\,t_a \exp\left(-x\sqrt{\frac{\omega}{2\alpha}}\right)}{\sec\left(\omega\tau - x\sqrt{\frac{\omega}{2\alpha}} - b\right)} \qquad 5$$

Where:

$$a = \sqrt{\frac{1}{2c^2+2c+1}} \qquad 6$$

$$b = \arctan\left(\frac{c}{c+1}\right) \qquad 7$$

and $$c = \sqrt{\frac{k\omega\rho c_p}{2h^2}} \qquad 8$$

The behavior of the analytical and corresponding numerical solutions are shown in Figure 2 for several different values of time, τ, calculated for a discretization with $\Delta x = 0.0025$ m and $\Delta\tau = 100$ sec. These calculations were performed for a semi-infinite slab of steel, $k = 60.5$ W/m/K, $\alpha = 1.77\times10^{-5}$, $h = 10.0$ W/m^2/K. The values needed to specify the ambient temperature, t_∞, are $\bar{t} = 300.0$ K, $t_a = 10.0$ K, and $\omega = 2\pi \times 24$ hours. The phase of the ambient temperature is specified such that the peak ambient temperature occurs at noon.

The plot in Figure 2 exhibits several features of note. It can be observed that, of the four times shown, high levels of heat flux into and out of the surface ($x = 0$) occur at noon and midnight, respectively. This is evident because high heat flux into the slab will result in a large

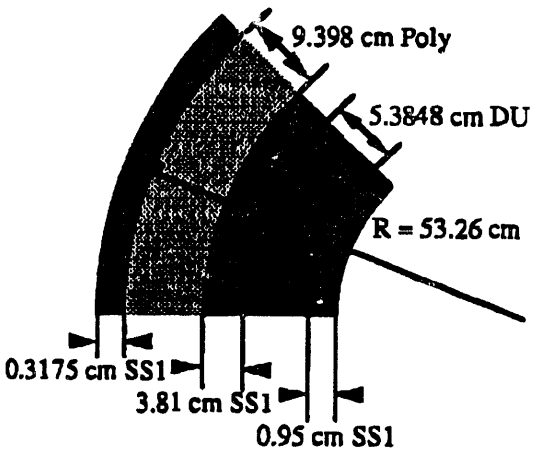

Drawing not to Scale

Figure 4: Schematic Drawing of Generic Truck Cask Wall

negative gradient in temperature near the surface of the slab. Furthermore, when the ambient temperature has returned to 300 K at both 6 AM and 6 PM, the surface flux is near zero (the slope of the temperature at the surface is approximately zero), due to the small temperature difference between the ambient fluid and the steel slab. Figure 2 also demonstrates the level of accuracy of the computational algorithm, as at most points the numerical simulation cannot be distinguished from the analytical solution. For this benchmark case, the semi-infinite slab is approximated by a slab five meters in width, and the data presented in Figure 2 demonstrates graphically that significant temperature variations do not propagate beyond this distance.

Figure 3 shows the L_2 error norm of the entire numerical solution in space and time (over an entire 24 hour cycle, and for the entire slab). The L_2 norm of the error is defined as:

$$L_2 = \frac{\Delta\tau\,\Delta x}{TX}\sqrt{\sum_{j=1}^{M}\sum_{i=1}^{N}\left[t_f(x_i,\tau_j) - t_n(x_i,\tau_j)\right]^2} \qquad 9$$

The values X and T represent the total length and time of the computation, respectively (five meters and twenty-four hours), and the subscripts f and n denote the analytical and numerical solutions, respectively. The L_2 norm error is calculated as a function of spatial discretization for several time steps. Figure 3 demonstrates the convergence of the algorithm, and suggests that the scheme will approach a single solution (equal to the analytical one) through subsequent refinement of spatial and temporal discretization. Temporal error is seen to propagate into the spatial solution; this effect is manifested in the form of a decrease in the magnitude of the slope of the error curve in Figure 3 when the spatial discretization is more refined than the temporal discretization.

Table 1: Thermal Properties of Materials

	Thermal Cond. W/m/K	Density kg/m³	Heat Cap. J/kg/K
SS1	13.85	7888.7	460.44
SS2	15.95	8027.0	502.3
DU	25.54	19293	131.85
Pb	35.13	11340	125.57
POLY	0.1454	941.11	1925.5
C/Cu	16.45	1849.0	2164.0

III. RESULTS

Since current spent fuel shipping cask designs are of two general types and sizes as dictated by the two major methods of transportation, road and rail, it was determined that examinations of both a generic Truck Cask (TC) and a generic Rail Cask (RC) were in order. The TC design and results will be discussed immediately, the RC will follow thereafter.

A. Truck Cask Analysis

The TC wall design appears in Figure 4. The cask wall of this design consists of five laminations, three of Stainless Steel (SS1), and one each of Depleted Uranium (DU) and Polypropylene (POLY). The stainless steel serves primarily as structural support, while the polypropylene is a neutron shield, and the depleted uranium acts as a gamma barrier. Figure 4, while not to scale, shows the dimensions of the cask wall as implemented in the subsequent analyses. An additional cask component not shown in Figure 4, which may or may not be present, is a solar shield, which also acts as a personnel barrier. The thermal properties of the various materials are central to the analysis which follows, so they are provided in Table 1. Table 1 also includes thermal properties for the RC design. Additionally, the subsequent analyses utilized an assumed convection coefficient of $h = 10$ W/m²/K. This value is frequently cited for natural convection from horizontal plates.[2,7]

The emissivities of the cask surface and the solar shield are not known quantities, as emissivities typically vary considerably with material type and surface characteristics. It is expected that the emissivities of the cask surface and shield will exist in the range 0.3 to 1.0. Differences in emissivity may cause significant changes in the relative importance of the *transient* thermal behavior of the cask. These changes may result in a greater difference between the overall maximum temperature profile and the regulatory solution.

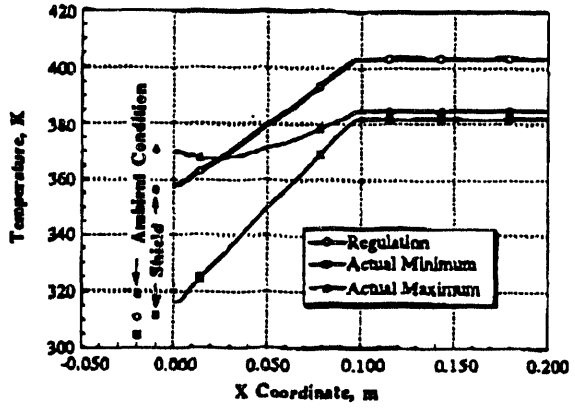

Figure 5: Truck Cask, Base Case
($\varepsilon_{surf} = 0.3$, $\varepsilon_{shield} = 1.0$)

A series of studies were undertaken to find the values of emissivity which resulted in a worst case scenario for the TC. The goal of performing analyses on permutations of solar shield and surface emissivities is to find the case in which the maximum portion of the cask wall is exposed to temperatures exceeding the regulatory calculation. It became evident that while all cases exhibit similar characteristics, the worst case is that illustrated in Figure 5, a TC with a black solar shield and a gray cask surface ($\varepsilon = 0.3$). This case not only involves the largest portion of cask above the regulatory temperature, but it also involves the smallest margin of compliance in the interior region of the cask, where the maximum temperature is somewhat less than 20 K below the regulatory condition. The term "margin of compliance" refers to the temperature difference by which the regulatory solution exceeds the realistic solution at the interior boundary of the cask wall. Thus, Figure 5 is identified as the base case for the remainder of the TC analysis, since it represents a worst-case scenario for the emissivity conditions.

The *actual* profiles in Figure 5 were calculated by monitoring the temperatures throughout the problem domain on the final, converged day of the simulation, and without regard to time of day, recording the minimum and maximum temperatures for each node in the solution. The regulatory condition is truly steady-state, so no such bounding solutions are necessary. The maximum, minimum and regulatory values of the ambient temperature and shield temperature are also displayed in the plot, however, little attention should be paid to the x-coordinates of these data points, as their spatial positions are not strictly specified.

The general behavior demonstrated in Figure 5 is typical of most solutions for the TC. The amplitude of the diurnal thermal wave is illustrated by the bounding minimum and maximum curves. It can be seen that the amplitude of the thermal wave decreases sharply in the region corresponding to the POLY neutron shield. This is

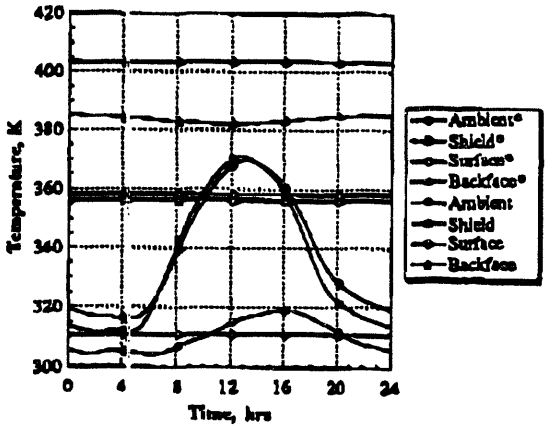

Figure 6: Truck Cask, Base Case, Diurnal Variation for Realistic Simulation and Regulatory Conditions (*)

due to the wave attenuating effect of materials with small thermal conductivities. The immediately obvious information demonstrated by Figure 5 is that, for at least part of the day, the temperature in the outer regions of the cask wall exceeds that temperature which is predicted when the regulatory condition is applied. However, in the regions inside the neutron shield, and for most of the neutron shield itself, the maximum temperature is bounded by the regulatory condition.

Figure 6 shows the temporal variation of temperature over a full twenty-four hours for the ambient condition, solar shield, cask surface and cask backface in a comparative analysis of the generic truck cask. It is interesting to note in Figure 6 that the peak shield temperature occurs just after noon, solar time, while the ambient temperature peak is at four in the afternoon. This indicates that insolation dominates the environmental heat transfer effects, and that the high solar flux is strictly responsible for the brief period during which the shield and cask surface exceed the regulatory solution. The cask surface is seen to vary essentially in phase with the solar shield temperature; this is due to the inability of the surface to communicate thermal energy freely to the greatest portion of the thermal mass of the cask, due to the insulating neutron shield. The plot in Figure 6 also demonstrates that the backface never exceeds the regulatory solution in the base case. Furthermore, the peak backface temperature occurs at approximately midnight, which implies that the thermal waves require a full twelve hours to propagate through the TC wall.

B. Rail Cask Analysis

The rail cask configuration is shown in Figure 7. The RC wall consists of four laminations, two of which are a slightly different alloy of stainless steel from that used in the TC, hereafter referred to as SS2. The neutron shield of the RC is composed of Concrete containing Copper fins (denoted subsequently as C/Cu) to aide the transfer of

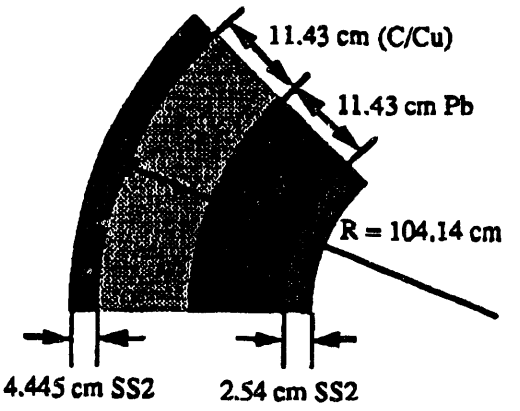

Drawing not to Scale

Figure 7: Schematic Drawing of Generic Rail Cask Wall

heat away from the spent fuel. The gamma shield is Lead (Pb). The dimensions of the various laminations, as well as the cask radius, appear in Figure 7.

Figure 8, the worst case for the RC, exhibits remarkably different characteristic temperature profiles as compared to those of the TC. The rather high thermal conductivity of the C/Cu neutron shield leads not only to a decrease in the thermal wave attenuation of the wall, but it also allows the entire mass of the cask wall to absorb the energy associated with the thermal waves. The end result of these phenomena is that the entire cask wall lies below the calculated regulatory profile. Also of note is the very small slope of the temperature profiles in each of the figures; this is a direct result of the high thermal conductivity across the entire wall.

Figure 9 demonstrates explicitly some of the key features of the RC wall design. The main feature of the RC, its higher thermal conductivity neutron shield, causes two major changes in the phase shift of the propagating thermal waves. First, the ability of the cask surface to communicate with the entire cask wall thermal mass allows the peak temperature of the surface to occur about three hours after the peak solar shield temperature. Additionally, the backface temperature is now more closely in phase with the surface temperature, with a phase lag of about two hours, because of the small time constant of the composite wall. The importance of these effects is in the fact that the entire cask wall absorbs and diminishes the effect of the diurnal transient, so that the surface temperature is now very much lower than the regulatory temperature, at all times.

Several other analyses were performed in order to examine the behavior of the TC and RC having introduced differences in cask geometry and composition. These analyses are presented in the report.[5] In general, it

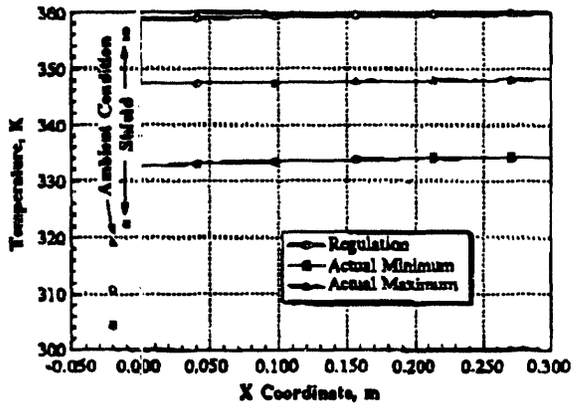

Figure 8: Rail Cask, Base Case ($\varepsilon_{surf} = 0.3$, $\varepsilon_{shield} = 1.0$)

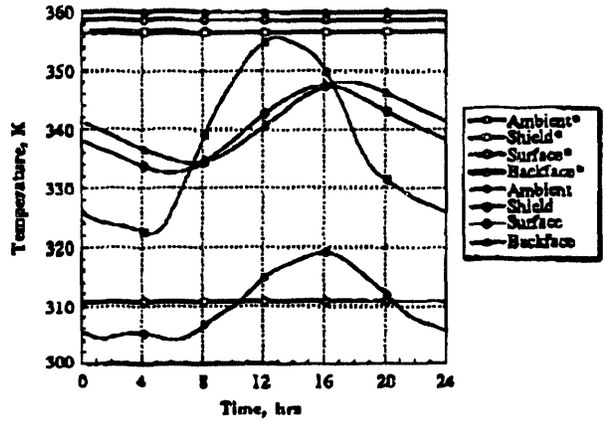

Figure 9: Rail Cask, Base Case, Diurnal Variation for Realistic Simulation and Regulatory Conditions (*)

was found that the base cases are representative of the behavior encountered for a wide variety of cask configurations. It was demonstrated that the maximum temperatures in the outer regions can exceed the corresponding regulatory solutions, but only by a few more degrees than the TC base case, at worst.

IV. CONCLUSIONS

The simulations performed in the course of this analysis have consistently and uniformly shown that the *interior* maximum wall temperatures of both the TC and RC fall well below those predicted when the steady-state implementation of the regulatory model is used. It has been shown that maximum temperatures near the surface of some cask designs, and at the solar shield, occasionally lie slightly above the regulatory prediction. These temperature differences are small and of short duration. It is also pointed out that the "realistic" conditions utilized in this study are conservative, as the temperature condition and the insolation condition are taken from two different locations, each the worst case out of all the available data. This means that while either condition may be encountered in principle, both conditions have never been observed to occur simultaneously. This conservativity enforces the calculated solutions as worst case limitations. Since this diurnal model is bounding, it is expected that no real situations will develop in which maximum wall temperatures exceed the regulatory calculation.

The analyses have made it clear that diurnal temperature variations which penetrate the cask wall have maxima substantially less than the corresponding regulatory solutions. Therefore, it is likely that vital cask structural components located interior to the neutron shielding, and the spent fuel itself, will not exceed the temperatures calculated even when a *transient* interpretation of 10CFR71 is used. However, this is not necessarily the case with regard to the outer regions of the cask wall. Therefore, some caution must be used in the evaluation of cask designs where external temperatures exceed regulatory limits predicted using a transient interpretation of 10CFR71. Particularly of interest is the temperature restriction involving the accessible surface of the cask. Care must be taken to ensure that proper levels of conservatism are used in such calculations, or it is conceivable that actual casks that meet the accessible surface limitation under the regulatory normal day conditions may fail to meet the same condition under circumstances involving real days with extreme temperatures and high insolation levels.

Finally, it was determined that the key factor in calculating the cask response to ambient conditions is the material composition of the neutron shield. Unlike typical structural materials (metals), and gamma shields (heavy metals), neutron shields can be made of quite a large variety of materials, having a wide range of thermal properties. Investigations using two potential shield choices, POLY and C/Cu, revealed a large variation in cask response between the materials. Furthermore, it was found that POLY is the limiting case as it may cause external transient temperatures to exceed those calculated using the regulatory normal condition by the largest margin observed, although *internal* temperatures remain below those predicted for the regulatory condition.

NOMENCLATURE

α	Thermal Diffusivity, m^2/s
c_p	Specific Heat, J/kg/K
∂	Partial Differential Operator, unity
Δ	Difference Operator, unity
ε	Emissivity, unity
h	Convection Heat Transfer Coefficient, $W/m^2/K$
k	Thermal Conductivity, W/m/K
q'''	Volumetric Heat Generation, W/m^3
q''	Heat Flux, W/m^2
r	Radial Position, m
ρ	Density, kg/m^3

t	Temperature, K
t_∞	Ambient Temperature, K
t_a	Amplitude of Temperature Cycle, K
t_f	Analytical Temperature Solution, K
t_n	Numerical Temperature Solution, K
$\bar{t}$	Mean Temperature, K
T	Total Time, s
τ	Time, s
ω	Angular Frequency, rad/s
X	Total Length, m

REFERENCES

1. Lake, W. H., "Modeling the Normal Thermal Environment," Proceedings of the 6th International Symposium on Packaging and Transportation of Radioactive Materials, pp. 1090-1097, West Berlin, November 10-14, 1980.

2. Brown, N. N., Gianoulakis, S. E., Lake, W. H., Comparison of 10 CFR 71 Normal Day Conditions With Bounding U. S. Hot Day Extremes, Sandia National Laboratories, SAND91-2255C, 1992.

3. Quinlan, F. T., Typical Meteorological Year User's Manual, National Climatic Data Center, Asheville, North Carolina, May, 1981.

4. Press, W. H., Flannery, B. P., Teukolsky, S. A., Vetterling, W. T., Numerical Recipes, FORTRAN Version, Cambridge University Press, 1989.

5. Manson, S. J., Gianoulakis, S. E., A Comparison of Spent Fuel Shipping Cask Response to 10 CFR 71 Normal Conditions and Realistic Hot Day Extremes, Sandia National Laboratories, SAND93-1771, to be published.

6. Gebhart, B., Heat Conduction and Mass Diffusion, McGraw-Hill Inc., 1993.

7. Incropera, F. P., DeWitt, D. P., Fundamentals of Heat and Mass Transfer, Second Edition, John Wiley & Sons, 1981.

DISCLAIMER

DATE
FILMED
4/18/94
END